Binding of amyloid β-peptide to ganglioside micelles is dependent on histidine-13

Mike P. WILLIAMSON*[1], Yu SUZUKI†[2], Nathan T. BOURNE*[2] and Tetsuo ASAKURA†

*Department of Molecular Biology and Biotechnology, University of Sheffield, Sheffield S10 2TN, U.K., and †Department of Biotechnology, Tokyo University of Agriculture and Technology, Tokyo 184-8588, Japan

Amyloid β-peptide (Aβ) is a major component of plaques in Alzheimer's disease, and formation of senile plaques has been suggested to originate from regions of neuronal membrane rich in gangliosides. Here we demonstrate using NMR on ^{15}N-labelled Aβ-(1–40) and Aβ-(1–42) that the interaction with ganglioside G_{M1} micelles is localized to the N-terminal region of the peptide, particularly residues His^{13} to Leu^{17}, which become more helical when bound. The key interaction is with His^{13}, which undergoes a G_{M1}-specific conformational change. The sialic acid residue of the ganglioside headgroup is important for determining the nature of the conformational change. The isolated pentasaccharide headgroup of G_{M1} is not bound, suggesting the need for a poly-anionic surface. Binding to heparin confirms this suggestion, since binding is of similar affinity but does not produce the same conformational changes in the peptide. A comparison of Aβ-(1–40) and Aβ-(1–42) indicates that binding to G_{M1} micelles is not related to oligomerization, which occurs at the C-terminal end. These results imply that binding to ganglioside micelles causes a transition from random coil to α-helix in the N-terminal region, leaving the C-terminal region unstructured.

Key words: Alzheimer's disease, amyloid, fibril, ganglioside, nuclear magnetic resonance (NMR), sialic acid.

INTRODUCTION

The brains of Alzheimer's disease patients are characterized by amyloid plaques, whose main constituent is the amyloid β-peptide (Aβ), which forms 'cross-β' fibrils [1]. This peptide ranges from 40 to 43 residues in length, with the difference being at the C-terminal end. Longer peptides are much more fibrillogenic [2]. All adult brains contain amyloid plaques, but in most individuals these are 'diffuse' and not apparently harmful; by contrast, in Alzheimer's disease sufferers, the plaques are fibrillar and are associated with dystrophic neurons. This, together with many other results, has suggested that it is the conversion from the diffuse into the fibrillar form that dictates disease progression. This has focused efforts on identifying the 'seed' from which fibrils are propagated, in what appears to be a nucleation-dependent process that involves a change in the conformation of the peptide [3]. Interestingly, the diffuse plaques are predominantly Aβ-(1–42) and the neuritic plaques predominantly Aβ-(1–40) [4].

A major debate has focused on whether the seed for fibril formation is formed in solution (possibly as an oligomer [5]) or on membrane surfaces. In recent years, much attention has focused on interactions between Aβ and gangliosides, particularly G_{M1} (Figure 1), which is one of the most abundant gangliosides in the brain, constituting approx. 20 % of brain gangliosides [6]. Gangliosides are sialic acid-containing glycosphingolipids with a role in synaptic transmission and signalling, and are found in high concentrations in neural cell membranes, particularly in synaptic membranes [7]. The finding that G_{M1}-bound Aβ is generated in human brain [8] has stimulated further studies in this area, including the recent results that ganglioside micelles stimulate aggregation and fibrillization of Aβ [9], that regional deposition of Aβ in the brain is induced by the local gangliosides [10], and that Aβ–G_{M1} binding in living cells takes place in a seed-dependent manner and induces cytotoxicity directly [11], and may be a mechanism common to many amyloidoses [12]. A particularly interesting line of research locates G_{M1}-rich membranes in cholesterol-rich lipid rafts [13,14], thereby suggesting how the amyloid deposits could affect neuronal membranes and signalling, and also why cholesterol and apolipoprotein E (which redistributes cholesterol in the brain) might be linked to Alzheimer's disease [15].

In the present paper, we describe NMR experiments aimed at characterizing the interactions between Aβ and ganglioside micelles. We have identified a small part of the peptide, residues 13–17, that we have demonstrated to be most crucial for substrate-specific interaction. A comparison of Aβ-(1–40) and Aβ-(1–42) suggests that Aβ-(1–42) forms oligomers in solution by interactions at the C-terminus, but that these are not related to G_{M1} binding. The relationship to seeding of amyloid plaques is discussed.

EXPERIMENTAL

Uniformly ^{15}N-labelled Aβ-(1–40) and Aβ-(1–42) were purchased from rPeptide (Athens, GA, U.S.A.), and gangliosides were purchased from Alexis Biochemicals (now Axxora U.K.), Nottingham, U.K. The purity of the gangliosides is quoted as >98 % by the manufacturer, but was not checked. All other reagents were from Sigma–Aldrich. The heparin used was the sodium salt (H4784).

Aβ-(1–40) solutions were prepared as described in [16]. In brief, the peptide was dissolved at a concentration of 200 μM in 10 mM NaOH with 1 min of sonication, and immediately frozen if required. Subsequently, the pH was adjusted to 7.2 with a minimal amount of 0.1 M HCl, and ^2H_2O was added to make approx. 200 μM peptide solution containing 10 % ^2H_2O. Solutions

Abbreviations used: Aβ, amyloid β-peptide; HSQC, heteronuclear single-quantum correlation.

[1] To whom correspondence should be addressed (email m.williamson@sheffield.ac.uk).

[2] These authors contributed equally to this work.

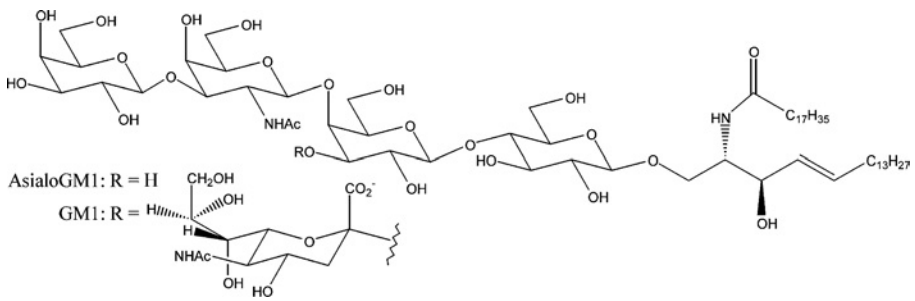

Figure 1 The structure of gangliosides G_{M1} and asialo-G_{M1}

prepared in this way were stable and showed no sign of aggregation for at least 1 week. By contrast, solutions made up in buffer aggregated much faster, often being almost entirely precipitated after 24 h. Aβ-(1–42) was pre-treated by dissolution in hexafluoropropan-2-ol and freeze-drying, before dissolving in 10 mM ammonium hydroxide, followed by adjustment of the pH to 7.2. These solutions started to aggregate and form fibrils immediately and were only usable for 2–3 days. Solutions of the commercial material directly into NaOH resulted in no NMR signal, indicating significant aggregation using this method. Stock solutions of gangliosides or heparin were prepared at high concentrations (approx. 100–200 mM), adjusted to pH 7.2 and added directly to the NMR tube. All NMR experiments were carried out on a Bruker DRX-500 equipped with a cryoprobe, and operated at 13 °C. ^{15}N HSQC (heteronuclear single-quantum correlation) experiments used gradient selection for water suppression and water flip-back pulses to minimize loss of magnetization through exchange and relaxation processes. The three-dimensional TOCSY-HSQC spectrum incorporated solvent suppression using gradients, with a 35 ms spin-lock at 8.3 kHz decoupler power. Processing of NMR data used FELIX (Accelrys, San Diego, CA, U.S.A.), and titration data were analysed using home-written scripts. Cross-peak intensities were measured within FELIX, transferred to a text file, and fitted to an exponential decay using a Marquardt non-linear least-squares fitting based originally on a Numerical Recipes algorithm. Binding constants were obtained by fitting to a standard equation using Excel (Microsoft).

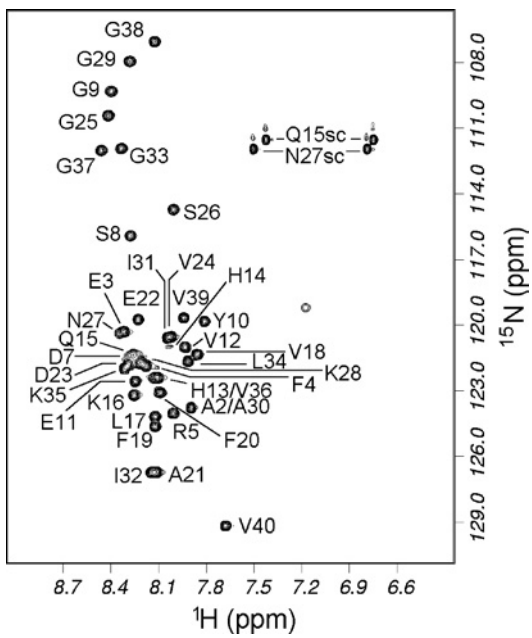

Figure 2 HSQC spectrum of ^{15}N-labelled Aβ-(1–40) in water, pH 7.2, 13 °C

The small unlabelled peak at (^{1}H = 7.2, ^{15}N = 119 p.p.m.) is probably an arginine side chain NH. Single-letter amino acid codes are used.

RESULTS

The HSQC spectrum of Aβ-(1–40) was assigned based on assignments described in [16] and kindly provided by Dr M. Zagorski (Department of Chemistry, Case Western Reserve University, Cleveland, Ohio, U.S.A.). Assignments were confirmed using a three-dimensional TOCSY-HSQC experiment, and proved to be very similar to published assignments [16]. The HSQC spectrum is shown in Figure 2. Almost all backbone signals are resolved. At 13 °C, all signals were found except for the N-terminal residue and His^6. His^{14} gives a weak signal, as expected because of its rapid amide exchange under these conditions [17]. The reason for the absence of His^6 in our HSQC spectra is less clear, but it was also not observable by Hou et al. [16]. On the basis of the chemical shifts, we concur with other authors [16,18] that the peptide is a random coil in aqueous solution. The majority of HSQC peaks in Aβ-(1–42) were assigned in the same way, but the assignment is somewhat less complete due to its rapid aggregation, which limits the time available for three-dimensional NMR experiments. The signals from Aβ-(1–42) have very similar chemical shifts to those of Aβ-(1–40) except at the C-terminus, implying that there are no significant conformational differences between them.

G_{M1} forms micelles with a critical micelle concentration in the low micromolar range [19]. Thus, at concentrations >100 μM, as used here, it is essentially 100 % micellar. On titration of G_{M1} micelles into Aβ-(1–40), chemical shift changes were seen in the NMR spectrum, as shown in Figure 3. The chemical shift changes were small, but are reproducible and specific, since many residues have essentially no change in shift. Smaller chemical shift changes have been demonstrated to be biologically relevant on many previous occasions [20,21]. Almost all of the chemical shift changes were in the N-terminal half of the peptide, and were close to potentially positively charged residues: Glu^3–Arg^5 (close to Arg^5 and His^6) and Val^{12}–Leu^{17} (close to His^{13}, His^{14} and Lys^{16}). However, the pK_a values of the three histidine residues are all approx. 6.5 [22]. Hence, at the pH of our measurements, 7.2, most of the histidine residues will be unprotonated. We therefore expect that the only residues significantly positively charged at this pH will be Arg^5 and Lys^{16}, together with Lys^{28}. This makes it unlikely that the chemical shift changes are due only to coulombic interactions with the single negative charge in the G_{M1} headgroup, the sialic acid. In order to confirm this, a further titration was carried out at an approximate physiological salt concentration (150 mM NaCl), which should markedly reduce purely coulombic

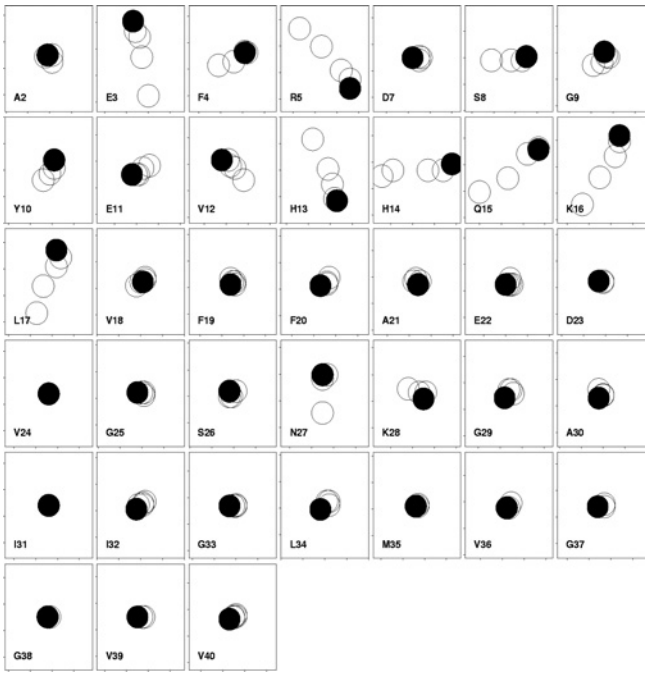

Figure 3 Chemical shift changes in Aβ-(1–40) on addition of G_{M1} to 200 μM peptide in water

Each box shows results for a different residue, with ^{1}H shifts horizontal (increasing left to right, total range $\pm$0.02 p.p.m.) and ^{15}N shifts vertical (increasing bottom to top, total range $\pm$0.1 p.p.m.). This representation therefore resembles the change seen in an HSQC spectrum, except that the directions of the axes are reversed. The start of the titration is indicated with a filled circle, and subsequent titrations are 1, 2, 4 and 8 equivalents of G_{M1}. The size of the circles approximates the experimental uncertainty. No data are shown for His^6 because it could not be observed. Single-letter amino acid codes are used.

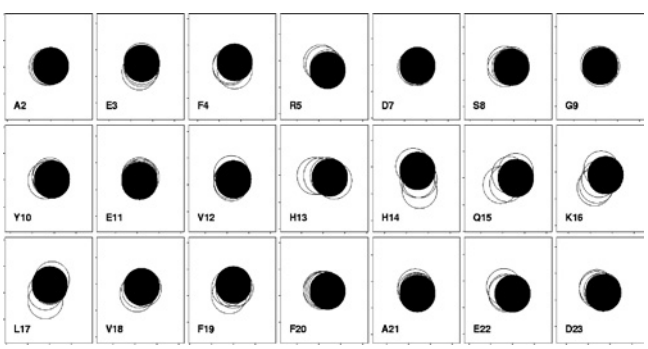

Figure 4 Chemical shift changes in Aβ-(1–40) on addition of G_{M1} to 200 μM peptide in 150 mM NaCl

Only the N-terminal residues are shown, because there were effectively no changes in the C-terminal residues. Titrations are 0, 1, 2, 4 and 6.6 equivalents of G_{M1}. Other conditions are as for Figure 3. Single-letter amino acid codes are used.

interactions in water. The results (Figure 4) showed reduced chemical shift changes, indicating a loss of affinity. Residues 14–17 still shift, but the changes seen in residues 3–13 are much reduced. This implies that, although some of the binding and the chemical shift changes are primarily coulombic in origin, others (and in particular the changes seen in residues 15–17) are much less so. We note that other authors have concluded that binding to G_{M1} is not primarily coulombic, although again there are clearly coulombic interactions [23–25].

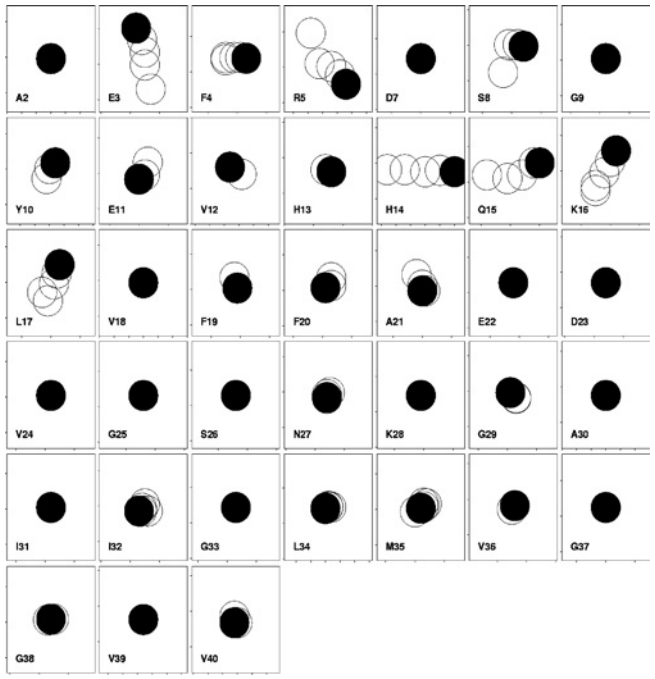

Figure 5 Chemical shift changes in Aβ-(1–40) on addition of asialo-G_{M1} to 200 μM peptide in water

Other conditions are as for Figure 3, except that the chemical shift ranges in each box are $\pm$0.015 p.p.m. for ^{1}H and $\pm$0.075 p.p.m. for ^{15}N. Single-letter amino acid codes are used.

A further titration of Aβ-(1–40) was carried out, using micelles of asialo-G_{M1} (Figure 1). The results are shown in Figure 5, in which the chemical shift ranges used in the plot are 75 % of those used for Figure 3, and show that chemical shift changes with asialo-G_{M1} were similar to those seen for G_{M1} but were reduced in magnitude for equivalent concentrations by approx. 25 %. A reduction is expected in the magnitude of the shift change, because asialo-G_{M1} is known to bind less tightly than G_{M1} to Aβ. The extent of the difference has been reported differently. Choo-Smith et al. [23] report no binding at all to asialo-G_{M1}, while a factor of 2 has also been reported [26]. Our data are in better agreement with the latter result [26]. The overall similarity of the chemical shift changes for G_{M1} and asialo-G_{M1} implies that the binding interactions are similar, although with some differences in the region of His^{13}–Gln^{15}. This result therefore also implies that the interaction is not dominated by coulombic forces, since asialo-G_{M1} has no charge in the headgroup.

In a further experiment, Aβ-(1–40) was titrated with heparin (Figure 6). The chemical shift changes again affected very similar residues to those affected by G_{M1}, although the size and direction of the change was in several cases markedly different (e.g. Arg^5, His^{13} and His^{14}). Heparin is a polyanionic polysaccharide (consisting mainly of 2-deoxy-2-sulphamino-α-D-glucose 6-sulphate, α-L-iduronic acid 2-sulphate, 2-acetamido-2-deoxy-α-D-glucose, β-D-glucuronic acid and α-L-iduronic acid in random order), but otherwise has little structural similarity to G_{M1} micelles. Despite its completely different covalent structure, and presumably its three-dimensional structure, it causes similar chemical shift changes in Aβ to those caused by ganglioside micelles. Hence, many of the changes must reflect a general conformational propensity of the peptide on binding to a surface, especially to one carrying a negative charge (although the overall similarity of results from asialo-G_{M1} imply that a negative charge is not essential).

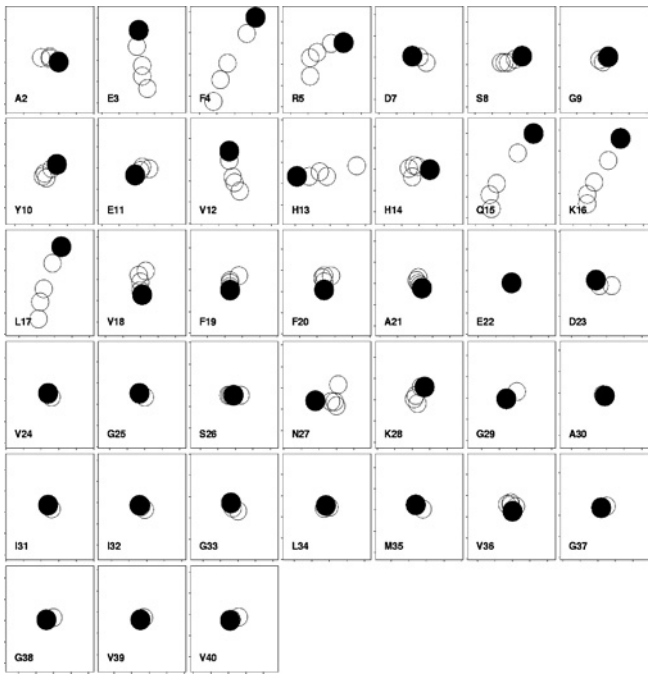

Figure 6 Chemical shift changes in Aβ-(1–40) on addition of heparin to 200 μM peptide in water

Other conditions are as for Figure 3, except that the chemical shift ranges are $\pm$0.05 p.p.m. for ^{1}H and $\pm$0.3 p.p.m. for ^{15}N. Single-letter amino acid codes are used.

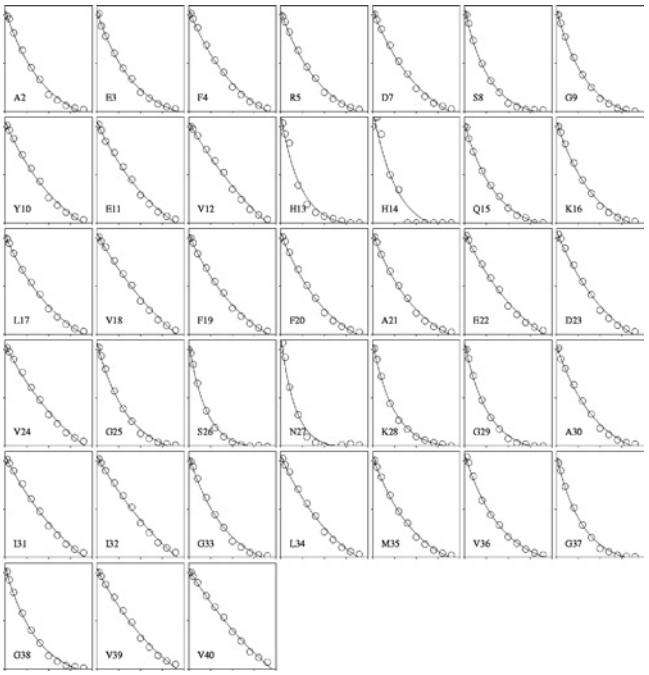

Figure 7 Intensity changes of HSQC peaks on addition of G_{M1} micelles to Aβ-(1–40)

The horizontal scale shows the molar ratio of G_{M1} to Aβ, with for each residue a range of 0–40 molar equivalents: the data are shown for 0, 1, 2, 4, 8, 12, 16, 20, 24, 28, 32 and 36 equivalents. The vertical scale shows the peak intensity relative to that in pure peptide, on a range from 0 to 100 %. The intensity changes are fitted to an exponential decay. Single-letter amino acid codes are used.

However, the exact structure adopted when bound, indicated by the direction of the chemical shift changes for residues Phe[4], Arg[5], Val[12] and His[13] in particular, depends on the substrate.

By contrast, Aβ-(1–40) was also titrated with the pentasaccharide headgroup of G_{M1}. No chemical shift changes were observed (results not shown), implying a lack of interaction, and therefore the requirement for an extended surface for efficient binding. A similar observation has been made previously [27].

The chemical shift changes for Gln[15], Lys[16] and Leu[17] on titration were in all cases similar, and show a reduction in chemical shift (i.e., an upfield shift) for both ^{1}H and ^{15}N. These changes are those expected for a change from random coil to α-helix, and in the opposite direction for those expected on going from random coil to β-sheet [28,29]. The results therefore imply that this region of the peptide becomes more helical on binding, but that the interacting region N-terminal to this sequence has a more complicated and substrate-specific conformational change.

The affinity of Aβ-(1–40) for G_{M1} micelles was estimated by fitting the chemical shift changes to a standard saturation curve [30]. The numerical result requires an assumption as to the number of G_{M1} molecules in a micelle. Here we have assumed an aggregation number of 310 [31], which produces a dissociation constant for a micelle of approx. 5 μM, in rough agreement with values produced by others for binding to vesicles containing G_{M1} [13,14,23]. This result implies that the fairly weak binding to G_{M1} does not act to concentrate Aβ directly (and therefore increase the local concentration of Aβ which might encourage fibrillization); rather, it acts to fix Aβ into a fibrillogenic conformation. When the dissociation constant is calculated for G_{M1} monomers, it is much weaker at approx. 1 mM. The dissociation constant for heparin (per disaccharide repeat) is similar, implying that the binding to gangliosides is not particularly strong, in agreement with results from other groups [32]. The calculations also imply that at 8 equivalents of G_{M1} (the maximum shown here), the shift changes are approx. 30 % of maximal. Thus, ^{1}HN chemical shift changes on 100 % binding to G_{M1} micelles are estimated to be approx. 0.06 p.p.m. for residues 15–17, implying that the bound structure is not fully helical, which would produce shift changes of approx. 0.2 p.p.m. [28].

During the course of the titration, reductions in peak intensity and increases in line width were seen in the HSQC spectrum. Such changes are expected due to the increased correlation time arising from binding to a large micelle, which reduces T_2 and therefore reduces intensity in multipulse experiments such as HSQC. For most protons, the increased line width and reduced intensity seen are consistent with a fast-exchange limit equilibrium between the free and micelle-bound forms: fast exchange is expected from the relatively weak binding affinity, which is in the low micromolar range. Thus, for the heparin titration, intensity changes were small and showed no clear variation along the sequence (except that the two C-terminal residues showed a lower intensity reduction, implying that there was little or no restriction in motional freedom arising from binding of the peptide to heparin). However, for the titrations with G_{M1}, intensity changes were large and markedly non-uniform along the sequence (Figure 7). One would expect the changes to be larger than with heparin because of the much longer correlation time of the G_{M1} micelles. The non-uniformity is consistent either with greater motional restriction at some sites or with exchange broadening. The latter explanation is less likely because the affinity is too weak to cause significant exchange broadening. As a way of handling the data, the intensities were fitted to an exponential curve (intensity

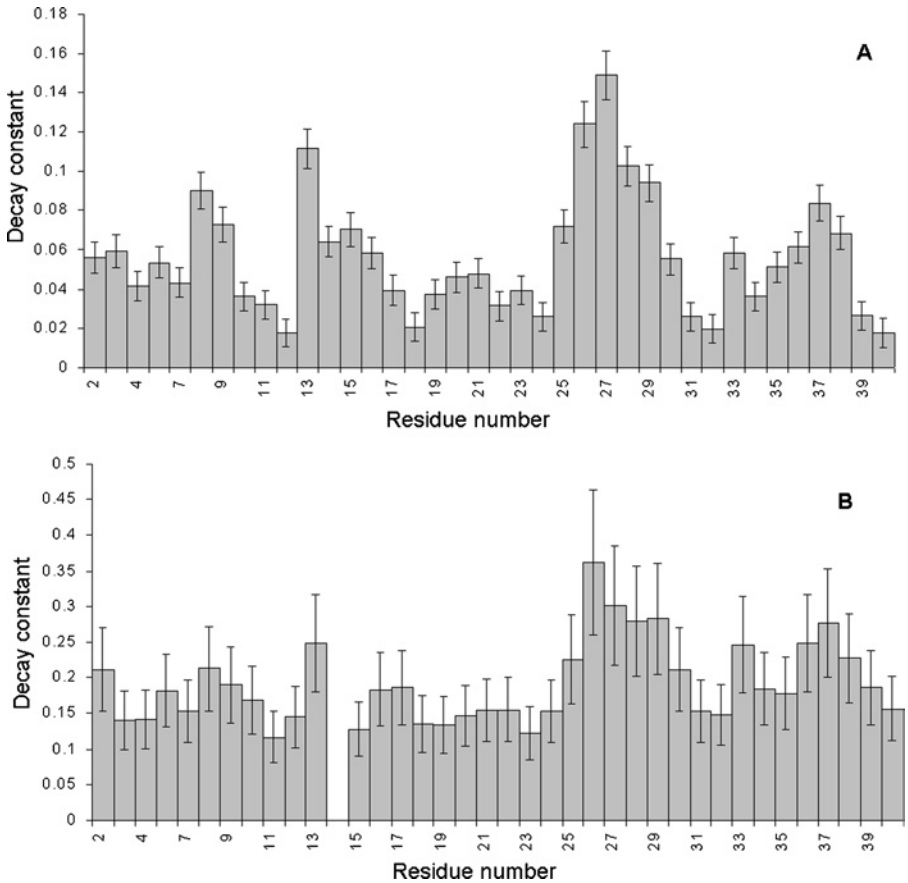

Figure 8 Loss of intensity during the titrations of (A) G_{M1} and (B) asialo-G_{M1} into Aβ-(1–40)

The bars show the decay constant from the exponential fits of the experimental data (Figure 7), with the estimated fitting error. The numerical values of the decay constants therefore have no direct meaning, but serve as a measure of the extent of intensity loss during the titration. Data for His^{14} are not shown in (**B**) because the intensity of His^{14} is too weak to allow fitting of the data.

against amount of G_{M1} added), the results of which are shown in Figure 8. For both G_{M1} and asialo-G_{M1}, the most dramatic decrease in intensity was for residues 26–28, despite the fact that these residues show only very small chemical shift changes. There was also faster broadening at the C-terminal end, around Gly^{37}. Loss of intensity can be caused by a large number of factors, all of which imply a change in conformation or environment. We therefore conclude that binding to G_{M1} micelles does affect the C-terminal part of the peptide, specifically around residues 27 and 37, even though only small or no chemical shift changes are seen here.

There are also marked decreases in intensity around His^{13} and Ser^{8} at the N-terminal end of the peptide on binding G_{M1}, which are smaller or absent on titration with asialo-G_{M1}. This implies a reduced interaction at these locations in asialo-G_{M1}, an observation that is consistent with the chemical shift changes described above, which were smaller and different for asialo-G_{M1} for Ser^{8}, Gly^{9}, His^{13} and Gln^{15}. Thus both chemical shift changes and line-broadening imply an interaction with the sialic acid group in the region of residues 8–15. HSQC experiments were also performed on Aβ-(1–42). This peptide differs from Aβ-(1–40) only by the presence of Ile^{41} and Ala^{42}. Immediately after separation of aggregates by treatment with hexafluoropropan-2-ol, followed by freeze-drying, sonication at high pH and adjustment to pH 7.2, HSQC spectra already indicated the presence of aggregated species, which increased in intensity with time (Figure 9). These signals were sharp and apparently in slow exchange with the monomer, and only affected C-terminal residues (from Gly^{33} onwards). We therefore conclude that the peptide forms small well-defined aggregates, probably dimers because of their sharpness, in a time-dependent manner, centred on the C-terminal. The sharpness of the oligomer signals is inconsistent with their being as large as hexamers.

Titrations of Aβ-(1–42) with G_{M1} showed chemical shift changes. The slow exchange between monomer and oligomer meant that we were able to monitor chemical shift changes for some of the C-terminal residues in both monomer and oligomer. We were therefore able to identify binding interactions for monomer and oligomer from the same solution. There were no significant chemical shift changes in either monomer or oligomer, for any of the residues showing signal splitting (i.e., Gly^{33} onwards), implying that the C-terminal end of the peptide does not interact with G_{M1} micelles, either as monomers or oligomers. The lack of binding of the oligomer is of interest in the light of recent reports that the fibrillogenic form of Aβ is soluble oligomers [5]. By contrast, residues in the N-terminal end show shift changes comparable with those observed for Aβ-(1–40), with the largest changes being for Tyr^{10}, Val^{12}, Lys^{16} and Leu^{17}. We noted that shift changes for His^{13} and Gln^{15} were not measurable due to signal overlap and poor solubility. We therefore conclude that Aβ-(1–42) binds to G_{M1} micelles in a similar way to Aβ-(1–40), and particularly in the region 10–17; and that it also undergoes

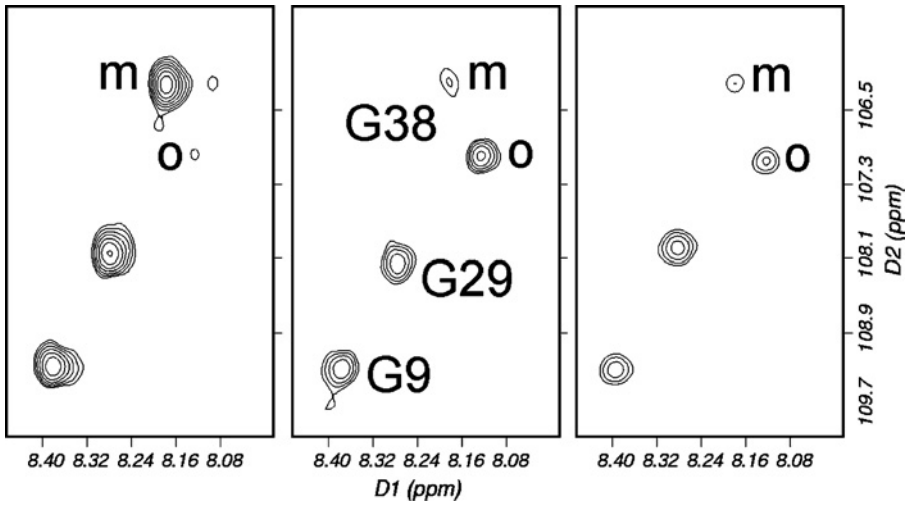

Figure 9 Titration of G_{M1} into Aβ-(1–42)

HSQC spectra of Aβ-(1–42) alone (left), with 8 molar equivalents of G_{M1} (centre) and 16 molar equivalents (right). The spectra were acquired sequentially, approx. 6 h apart. The signals for Gly^{9} and Gly^{29} are barely affected. The signal for Gly^{38} is also not affected by the addition of G_{M1}, but there is an independent and time-dependent loss of the signal from monomer (marked m) and increase of a signal from an oligomeric species (marked o). All signals are starting to decrease in the final spectrum because of precipitation of aggregates. Single-letter amino acid codes are used.

a dimerization or aggregation at the C-terminal end, which is independent of any binding to G_{M1}.

DISCUSSION

There have been a large number of conformational studies of Aβ. Many of these are in unphysiological solvents or in SDS or lipid micelles, which are well known to have a tendency to push peptides towards helical structures. It is therefore not surprising to find that these studies tend to report helical conformations for Aβ. However, studies in water have suggested random coil states [16,18], a conclusion with which we agree.

In the present study we demonstrate binding in the low micromolar range to G_{M1}, asialo-G_{M1} and heparin, but no measurable binding to the isolated G_{M1} headgroup. Several experiments (both ours and those of others [33]) have demonstrated that although there may be a coulombic element to the binding, the interactions are not limited to coulombic ones. Our results are therefore relevant to the physiological situation where the salt concentration is higher and coulombic interactions are weaker.

The chemical shift changes reported here demonstrate binding of Aβ to G_{M1} micelles, which is localized to the N-terminal half of the peptide. We confirm that binding to asialo-G_{M1} is weaker, specifically with differences around residues 12–15. This conclusion is radically different from one resulting from another NMR study [34]. However, that study was carried out using SDS micelles which may explain the difference in results compared with our present study. Binding to heparin also involves the same residues, although the chemical shift changes (and therefore presumably the interactions and conformational changes on binding) are different. Our results therefore agree with the consensus of opinion, which is that high-affinity binding is directed to the N-terminal end of the Aβ peptide [26]. For binding to heparin, the region 12–17 has been identified previously [33,35], and this region has also been demonstrated to be important for attachment to microglial cells and for neurotoxicity [36]. There is no binding to isolated pentasaccharide headgroups. The results therefore imply that Aβ binds to a range of surfaces in a similar way and with similar affinity, the binding being at the N-terminal end of the peptide.

Chemical shift changes (particularly of ^{15}N and ^{1}HN) are notoriously difficult to relate to specific conformational changes. However, there is wide agreement that helical regions have higher field ^{15}N and ^{1}HN shifts than random coil. The results reported here therefore imply that the short region from Gln^{15} to Leu^{17} becomes more helical on binding, to G_{M1}, asialo-G_{M1} and heparin. It is perhaps significant that this is exactly the same region identified above as being important for neurotoxicity [36]. The region C-terminal to Leu^{17} has little or no observable conformational change. Intensity changes did however suggest some interaction in this part of the peptide, particularly around residues 27 and 37.

A comparison of chemical shift changes in Aβ on addition of G_{M1} micelles compared with asialo-G_{M1} or heparin implies that His^{13} interacts specifically with the sialic acid moiety. Because previous studies have identified the sialic acid as being important for the growth of amyloid fibres [10,13,37], the results imply that His^{13} binding may play an important role in fibrillogenesis. Indeed, His^{13} has been identified previously as crucial for rapid fibrillization [38]. It is relevant to note that rats, which differ in their Aβ from humans in only three positions (mutants R5G, Y10F and H13R), do not form cerebral Aβ [39].

Comparison of chemical shift changes in Aβ-(1–40) and Aβ-(1–42) implies that binding to G_{M1} micelles is located at the N-terminal end, whereas the C-terminal end plays no part in binding, but does lead to oligomerization in solution. We note that residues 1–28 alone are sufficient for formation of structured aggregates, but do not form fibrils [40]. The results therefore suggest that the N-terminal binding of the peptide to G_{M1} may provide the initial fibrillogenic seed, but that the C-terminus is required for propagation into fibrils.

This raises the question of what the present study implies about the formation of amyloid fibres *in vivo*. The present study is consistent with the seeding/nucleation amyloid cascade model of Alzheimer's disease. By contrast, it implies that soluble Aβ aggregates, currently a very popular topic of study [5], may be off-pathway intermediates with no direct involvement in plaque formation. There is, however, a recent report [41] that Aβ polymers are found associated with lipid rafts in mouse brain, but that oligomers are found particularly at axon termini. It is therefore

possible that both modes of polymerization operate at the same time, in different regions of the brain. Multiple assembly pathways would be no surprise [42].

The present study also implies that the fibrillogenic seed nucleus involves an interaction of His^{13} with the sialic acid moiety of G_{M1}. Aβ can bind to other non-fibrillogenic surfaces (heparin, for example), but without inducing the same structural change in Aβ. This implies that binding of Aβ in other conformations may merely lead to build-up of Aβ without the formation of fibrils – in other words, to diffuse plaques. Indeed, this could provide an explanation of why Aβ-(1–42), which is less soluble than Aβ-(1–40) and speeds up fibrillogenesis [38], surprisingly tends to be found in diffuse rather than neuritic plaques [4]. We suggest that it binds and aggregates so rapidly that it does not have time to rearrange into the correct conformation to form the required seed. This suggestion is consistent with our observation that oligomerization of Aβ-(1–42) is rapid and independent of G_{M1} binding, and occurs in a different region of the peptide. It could also provide an explanation of the observation that the amount of soluble Aβ oligomer correlates with synaptic loss better than the amount of insoluble Aβ does [43]: it may be that deposition of Aβ in the correct conformation requires multiple equilibration between soluble and insoluble forms. The formation of fibrils is thus seen to be a fine balance between over-rapid deposition (leading to diffuse plaques) and inadequate deposition (leading to small and non-aggressive plaques). In partial support of this argument, we note that treatment of transgenic mice (which develop Alzheimer's disease-like symptoms) with anti-Aβ antibody not only leads to a reduction in plaques (implying reversible binding of Aβ to plaques *in vivo*), but also produces a reduction in neuritic damage, implying that the neuritic damage is a consequence of the plaques [44].

We thank the BBSRC (Biotechnology and Biological Sciences Research Council) for a studentship (N. T. B.) and for the award of a Japan Partnership Award to M. P. W. We thank the Wellcome Trust and BBSRC for grants for spectrometer and cryoprobe purchase.

REFERENCES

1 Kirschner, D. A., Abraham, C. and Selkoe, D. J. (1986) X-ray diffraction from intraneuronal paired helical filaments and extraneuronal amyloid fibers in Alzheimer disease indicates cross-β conformation. Proc. Natl. Acad. Sci. U.S.A. **83**, 503–507

2 Jarrett, J. T., Berger, E. P. and Lansbury, P. T. (1993) The carboxy terminus of the β-amyloid protein is critical for the seeding of amyloid formation. Biochemistry **32**, 4693–4697

3 Huang, T. H. J., Yang, D. S., Fraser, P. E. and Chakrabartty, A. (2000) Alternate aggregation pathways of the Alzheimer β-amyloid peptide. J. Biol. Chem. **275**, 36436–36440

4 Esiri, M. M. (2001) The neuropathology of Alzheimer's disease. In Neurobiology of Alzheimer's Disease (Allen, S. J., ed.), pp. 33–53, Oxford University Press, Oxford

5 Cleary, J. P., Walsh, D. M., Hofmeister, J. J., Shankar, G. M., Kuskowski, M. A., Selkoe, D. J. and Ashe, K. H. (2005) Natural oligomers of the amyloid-protein specifically disrupt cognitive function. Nat. Neurosci. **8**, 79–84

6 Kracun, I., Rösner, H., Cosovic, C. and Stavljenic, A. (1984) Topographical atlas of the gangliosides of the adult human brain. J. Neurochem. **43**, 979–989

7 Nagai, Y. (1995) Functional roles of gangliosides in bio-signaling. Behav. Brain Res. **66**, 99–104

8 Yanagisawa, K., Odaka, A., Suzuki, N. and Ihara, Y. (1995) G_{M1} ganglioside-bound amyloid β-protein (Aβ): a possible form of preamyloid in Alzheimer's disease. Nat. Med. **1**, 1062–1066

9 Yamamoto, N., Hasegawa, K., Matsuzaki, K., Naiki, H. and Yanagisawa, K. (2004) Environment- and mutation-dependent aggregation behavior of Alzheimer amyloid β-protein. J. Neurochem. **90**, 62–69

10 Yamamoto, N., Hirabayashi, Y., Amari, M., Yamaguchi, H., Romanov, G., van Nostrand, W. E. and Yanagisawa, K. (2005) Assembly of hereditary amyloid β-protein variants in the presence of favorable gangliosides. FEBS Lett. **579**, 2185–2190

11 Wakabayashi, M., Okada, T., Kozutsumi, Y. and Matsuzaki, K. (2005) G_{M1} ganglioside-mediated accumulation of amyloid β-protein on cell membranes. Biochem. Biophys. Res. Commun. **328**, 1019–1023

12 Gellermann, G. P., Appel, T. R., Tannert, A., Radestock, A., Hortschansky, P., Schroeckh, V., Leisner, C., Lutkepohl, T., Shtrasburg, S., Rocken, C. et al. (2005) Raft lipids as common components of human extracellular amyloid fibrils. Proc. Natl. Acad. Sci. U.S.A. **102**, 6297–6302

13 Kakio, A., Nishimoto, S., Yanagisawa, K., Kozutsumi, Y. and Matsuzaki, K. (2002) Interactions of amyloid β-protein with various gangliosides in raft-like membranes: importance of G_{M1} ganglioside-bound form as an endogenous seed for Alzheimer amyloid. Biochemistry **41**, 7385–7390

14 Kakio, A., Nishimoto, S., Yanagisawa, K., Kozutsumi, Y. and Matsuzaki, K. (2001) Cholesterol-dependent formation of G_{M1} ganglioside-bound amyloid β-protein, an endogenous seed for Alzheimer amyloid. J. Biol. Chem. **276**, 24985–24990

15 Wolozin, B. (2001) A fluid connection: cholesterol and Aβ. Proc. Natl Acad. Sci. U.S.A. **98**, 5371–5373

16 Hou, L. M., Shao, H. Y., Zhang, Y. B., Li, H., Menon, N. K., Neuhaus, E. B., Brewer, J. M., Byeon, I. J. L., Ray, D. G., Vitek, M. P. et al. (2004) Solution NMR studies of the Aβ-(1–40) and Aβ-(1–42) peptides establish that the Met^{35} oxidation state affects the mechanism of amyloid formation. J. Am. Chem. Soc. **126**, 1992–2005

17 Bai, Y. W., Milne, J. S., Mayne, L. and Englander, S. W. (1993) Primary structure effects on peptide group hydrogen exchange. Proteins: Struct., Funct., Genet. **17**, 75–86

18 Zhang, S., Iwata, K., Lachenmann, M. J., Peng, J. W., Li, S., Stimson, E. R., Lu, Y., Felix, A. M., Maggio, J. E. and Lee, J. P. (2000) The Alzheimer's peptide Aβ adopts a collapsed coil structure in water. J. Struct. Biol. **130**, 130–141

19 Basu, A. and Glew, R. H. (1985) Characterization of the activation of rat liver β-glucosidase by sialosylgangliotetraosylceramide. J. Biol. Chem. **260**, 3067–3073

20 Morrison, J., Yang, J. C., Stewart, M. and Neuhaus, D. (2003) Solution NMR study of the interaction between NTF2 and nucleoporin FxFG repeats. J. Mol. Biol. **333**, 587–603

21 Laguri, C., Phillips-Jones, M. K. and Williamson, M. P. (2003) Solution structure and DNA binding of the effector domain from the global regulator PrrA (RegA) from *Rhodobacter sphaeroides*: insights into DNA binding specificity. Nucleic Acids Res. **31**, 6778–6787

22 Ma, K., Clancy, E. L., Zhang, Y. B., Ray, D. G., Wollenberg, K. and Zagorski, M. G. (1999) Residue-specific pK_a measurements of the β-peptide and mechanism of pH-induced amyloid formation. J. Am. Chem. Soc. **121**, 8698–8706

23 Choo-Smith, L. P., Garzon-Rodriguez, W., Glabe, C. G. and Surewicz, W. K. (1997) Acceleration of amyloid fibril formation by specific binding of Aβ–(1–40) peptide to ganglioside-containing membrane vesicles. J. Biol. Chem. **272**, 22987–22990

24 McLaurin, J., Franklin, T., Fraser, P. E. and Chakrabartty, A. (1998) Structural transitions associated with the interaction of Alzheimer β-amyloid peptides with gangliosides. J. Biol. Chem. **273**, 4506–4515

25 Bokvist, M., Lindstrom, F., Watts, A. and Gröbner, G. (2004) Two types of Alzheimer's β-amyloid -(1–40) peptide membrane interactions: Aggregation preventing transmembrane anchoring versus accelerated surface fibril formation. J. Mol. Biol. **335**, 1039–1049

26 Ariga, T., Kobayashi, K., Hasegawa, A., Kiso, M., Ishida, H. and Miyatake, T. (2001) Characterization of high-affinity binding between gangliosides and amyloid β-protein. Arch. Biochem. Biophys. **388**, 225–230

27 Choo-Smith, L. P. and Surewicz, W. K. (1997) The interaction between Alzheimer amyloid β-(1–40) peptide and ganglioside G_{M1}-containing membranes. FEBS Lett. **402**, 95–98

28 Williamson, M. P. (1990) Secondary structure dependent chemical shifts in proteins. Biopolymers **29**, 1428–1431

29 Xu, X. P. and Case, D. A. (2002) Probing multiple effects on ^{15}N, $^{13}C\alpha$, $^{13}C\beta$, and $^{13}C'$ chemical shifts in peptides using density functional theory. Biopolymers **65**, 408–423

30 Charlton, A. J., Baxter, N. J., Khan, M. L., Moir, A. J. G., Haslam, E., Davies, A. P. and Williamson, M. P. (2002) Polyphenol/peptide binding and precipitation. J. Agric. Food Chem. **50**, 1593–1601

31 Cantu, L., Corti, M., Del Favero, E., Muller, E., Raudino, A. and Sonnino, S. (1999) Thermal hysteresis in ganglioside micelles investigated by differential scanning calorimetry and light-scattering. Langmuir **15**, 4975–4980

32 Kakio, A., Nishimoto, S. I., Kozutsumi, Y. and Matsuzaki, K. (2003) Formation of a membrane-active form of amyloid β-protein in raft-like model membranes. Biochem. Biophys. Res. Commun. **303**, 514–518

33 McLaurin, J. and Fraser, P. E. (2000) Effect of amino-acid substitutions on Alzheimer's amyloid-β peptide–glycosaminoglycan interactions. Eur. J. Biochem. **267**, 6353–6361

34 Mandal, P. K. and Pettegrew, J. W. (2004) Alzheimer's disease: NMR studies of asialo (G_{M1}) and trisialo (GT1b) ganglioside interactions with Aβ-(1–40) peptide in a membrane mimic environment. Neurochem. Res. **29**, 447–453

35 Brunden, K. R., Richter-Cook, N. J., Chaturvedi, N. and Frederickson, R. C. A. (1993) pH-dependent binding of synthetic β-amyloid peptides to glycosaminoglycans. J. Neurochem. **61**, 2147–2154

36 Giulian, D., Haverkamp, L. J., Yu, J. H., Karshin, M., Tom, D., Li, J., Kazanskaia, A., Kirkpatrick, J. and Roher, A. E. (1998) The HHQK domain of β-amyloid provides a structural basis for the immunopathology of Alzheimer's disease. J. Biol. Chem. **273**, 29719–29726
37 Matsuzaki, K. and Horikiri, C. (1999) Interactions of amyloid β-peptide -(1–40) with ganglioside-containing membranes. Biochemistry **38**, 4137–4142
38 Kirkitadze, M. D., Condron, M. M. and Teplow, D. B. (2001) Identification and characterization of key kinetic intermediates in amyloid β-protein fibrillogenesis. J. Mol. Biol. **312**, 1103–1119
39 Selkoe, D. J. (1989) Biochemistry of altered brain proteins in Alzheimer's disease. Annu. Rev. Neurosci. **12**, 463–490
40 Yip, C. M. and McLaurin, J. (2001) Amyloid-β peptide assembly: a critical step in fibrillogenesis and membrane disruption. Biophys. J. **80**, 1359–1371
41 Kokubo, H., Kayed, R., Glabe, C. G., Saido, T. C., Iwata, N., Helms, J. B. and Yamaguchi, H. (2005) Oligomeric proteins ultrastructurally localize to cell processes, especially to axon terminals with higher density, but not to lipid rafts in Tg2576 mouse brain. Brain Res. **1045**, 224–228
42 Goldsbury, C., Frey, P., Olivieri, V., Aebi, U. and Müller, S. A. (2005) Multiple assembly pathways underlie amyloid-β fibril polymorphisms. J. Mol. Biol. **352**, 282–298
43 Walsh, D. M., Klyubin, I., Fadeeva, J. V., Rowan, M. J. and Selkoe, D. J. (2002) Amyloid-β oligomers: their production, toxicity and therapeutic inhibition. Biochem. Soc. Trans. **30**, 552–557
44 Brendza, R. P., Bacskai, B. J., Cirrito, J. R., Simmons, K. A., Skoch, J. M., Klunk, W. E., Mathis, C. A., Bales, K. R., Paul, S. M., Hyman, B. T. and Holtzman, D. M. (2005) Anti-Aβ antibody treatment promotes the rapid recovery of amyloid-associated neuritic dystrophy in PDAPP transgenic mice. J. Clin. Invest. **115**, 428–433

Received 20 February 2006/30 March 2006; accepted 21 April 2006
Published as BJ Immediate Publication 21 April 2006, doi:10.1042/BJ20060293